

QCD transition line from strangeness fluctuations

**Piyush Kumar,^{a,*} Szabolcs Borsányi,^a Zoltán Fodor,^{a,b,c,d} Jana N. Guenther,^a
Paolo Parotto,^e Attila Pásztor^c and Chik Him Wong^a**

^a*Department of Physics, University of Wuppertal, Gausstr. 20, D-42119, Wuppertal, Germany*

^b*Department of Physics, Pennsylvania State University, State College, PA 16801, USA*

^c*Institute for Theoretical Physics, ELTE Eötvös Loránd University, Pázmány P. sétány 1/A, H-1117 Budapest, Hungary*

^d*Jülich Supercomputing Centre, Forschungszentrum Jülich, D-52425 Jülich, Germany*

^e*Dipartimento di Fisica, Università di Torino and INFN Torino, Via P. Giuria 1, I-10125 Torino, Italy*

E-mail: kumar@uni-wuppertal.de

Mapping the QCD phase diagram at large density remains challenging due to the complex action problem in lattice simulations. Using simulations at imaginary baryon chemical potential (μ_B), we observe that, under the strangeness-neutrality condition, both the strangeness chemical potential (μ_S/μ_B) and the strangeness susceptibility (χ_2^S) take on constant values at the chiral transition across varying μ_B . We present new lattice data to extrapolate contours of constant μ_S/μ_B or χ_2^S to finite baryon chemical potential. These proxies are shown to be only mildly affected by criticality and finite-volume effects, and their continuum limits up to $\mu_B = 400$ MeV agree well with existing determinations of the chiral transition and with the hadron resonance gas model.

*The 42nd International Symposium on Lattice Field Theory (LATTICE2025)
2-8 November 2025
Tata Institute of Fundamental Research, Mumbai, India*

*Speaker

1. Introduction

The phase structure of Quantum Chromodynamics (QCD) at large baryochemical potential remains elusive. Lattice studies using finite size scaling at zero chemical potential have established the transition between the hadronic matter and quark gluon plasma to be a smooth crossover [1] occurring around $T_c = 156 - 158$ MeV for physical quark masses [2, 3]. The nature of this phase transition at large density, however, remains an open question. Several Effective Field Theory (EFT) approaches to QCD predict the transition to be of first order at large chemical potential [4][5]. This suggests the existence of a second order critical point where the first order transition line originating from the μ_B -axis ends and the transition becomes a crossover. The search for the signatures of this critical point has attracted considerable attention from both the experimental and theoretical communities. On the theoretical side, the wide variability of the EFT and model based estimates for the critical endpoint calls for a first principles study through lattice computation. However, direct lattice simulations at finite chemical potential are hampered by the notorious *sign problem*. Due to the complex nature of the action at finite chemical potentials, the Boltzmann weight e^{-S} loses its probabilistic interpretation and the importance sampling breaks down. A common approach to circumvent this difficulty and to study the thermodynamics of QCD at finite density is to employ the Taylor series expansion of the thermodynamic observables around zero chemical potential.

The primary observables for studying the chiral transition are the chiral condensate and its associated susceptibility, from which the transition temperature is determined and systematically extrapolated to finite chemical potential. In this contribution, we motivate the use of the constant curves of the strangeness susceptibility, χ_2^S and the ratio of strange to baryon chemical potentials, μ_S/μ_B , along the strangeness neutral line, as proxies for the QCD transition line.

2. Proxies for the QCD transition

The low temperature phase of QCD is dominated by color singlet bound states, i.e., hadrons such as nucleons and pions. In particular, pions are the light Goldstone bosons emerging from spontaneous symmetry breaking of the approximate chiral symmetry. On the other hand, the high temperature phase is characterized by deconfined quarks and gluons as the degrees of freedom and by the restoration of chiral symmetry. The chiral condensate defined as the first derivative of the free energy density with respect to the light quark masses serves as the (pseudo) order parameter for the chiral transition. On the lattice, we calculate the condensate and its fluctuation—the chiral susceptibility—as functions of the temperature and identify the transition temperature with the peak of the susceptibility. The corresponding expressions for these observables read:

$$\langle \bar{\psi}\psi \rangle = \frac{T}{V} \frac{\partial \log Z}{\partial m_{ud}}, \quad \chi_{\bar{\psi}\psi} = \frac{T}{V} \frac{\partial^2 \log Z}{\partial m_{ud}^2} \quad (1)$$

The chiral condensate and susceptibility contain both additive and multiplicative UV divergences and thus need to be renormalized. One possible renormalization prescription is given by:

$$\langle \bar{\psi}\psi \rangle_{ud,R} = -\frac{m_{ud}}{f_\pi^4} \left[\langle \bar{\psi}\psi \rangle_{ud,T} - \langle \bar{\psi}\psi \rangle_{ud,T=0} \right], \quad \chi_{\bar{\psi}\psi,R} = \frac{m_{ud}^2}{f_\pi^4} \left[\chi_{\bar{\psi}\psi,T} - \chi_{\bar{\psi}\psi,T=0} \right] \quad (2)$$

where f_π is the pion decay constant. The observables central to this work are the strangeness susceptibility, χ_2^S and the strange chemical potential, μ_S/μ_B evaluated at the strangeness-neutral point, $\langle n_S \rangle \equiv \chi_1^S = 0$. The strangeness number density and the susceptibility are defined as:

$$\langle n_S \rangle \equiv \chi_1^S = \frac{T}{V} \frac{\partial \log Z}{\partial \mu_S}, \quad \chi_2^S = \frac{T}{V} \frac{\partial^2 \log Z}{\partial \mu_S^2} \quad (3)$$

We start with an empirical observation based on the $48^3 \times 12$ lattice simulation data set with 4-stout improved staggered action at zero and various imaginary chemical potentials. Under the condition of strangeness neutrality, the peak of $\chi_{\bar{\psi}\psi,R}$ corresponds to a constant value of both χ_2^S and μ_S/μ_B , independent of the (imaginary) chemical potential as illustrated in Fig. 1.

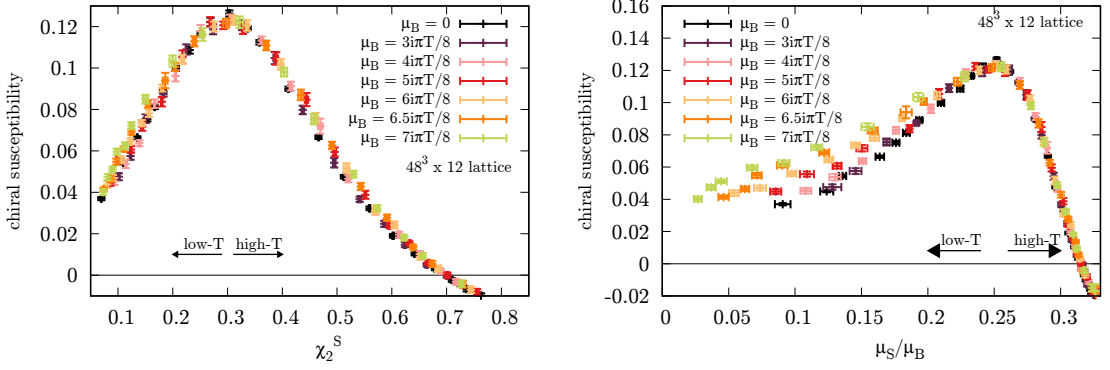


Figure 1: Renormalized chiral susceptibility as a function of strangeness susceptibility, χ_2^S (left) and the ratio of strange and baryon chemical potential, μ_S/μ_B (right) for various imaginary baryochemical potentials evaluated at the strangeness neutral point on a $48^3 \times 12$ lattice.

This suggests that these observables take nearly universal values defined by the peak of the chiral susceptibility: $\chi_2^S = \text{const.} \approx 0.3$ and $\mu_S/\mu_B = \text{const.} \approx 0.25$. Note that both χ_2^S and μ_S/μ_B are monotonic in temperature, which is required in order to identify the peak of $\chi_{\bar{\psi}\psi}(\chi_2^S)$ and $\chi_{\bar{\psi}\psi}(\mu_S/\mu_B)$ as the transition. The apparent collapse of curves for different imaginary chemical potentials persists even for chemical potential values very close to the Roberge-Weiss critical point at $\mu_B/T = i\pi$, indicating that for these proxies, non-singular behavior dominates in the vicinity of the critical point. In the following, using the quark meson model, we argue that the strangeness neutrality condition suppresses the coupling of χ_2^S to the singular fluctuations associated with a critical point. In this model, the quarks couple to the critical σ mode by means of a Yukawa term:

$$\mathcal{L}_{\sigma\bar{q}q} = G\sigma \sum_{i=u,d,s} \bar{q}_i q_i \quad (4)$$

where coupling constant G is the same for all three quark flavors due to $SU(3)_f$ symmetry. Following [6][7], we compute the critical contribution to the strangeness susceptibility due to coupling with the σ mode $\chi_2^{S(crit)}$, both for $\mu_S = 0$ and for strangeness neutrality, $n_S = 0$ which as we showed corresponds to $\mu_S \approx 0.25\mu_B$. The central quantity to compute is the flavor-flavor correlation (ij) between net fluctuations of net quark number:

$$\langle \Delta N^i \Delta N^j \rangle = V \int_p \int_k \langle \delta n_p^i \delta n_k^j \rangle \quad (5)$$

with

$$V\langle\delta n_p^i\delta n_k^j\rangle = \frac{G^2}{m_\sigma^2 T} \frac{4m_i m_j}{E_p^i E_k^j} \quad (6)$$

$$\times [n_p^{i,+}(1-n_p^{i,+}) - n_p^{i,-}(1-n_p^{i,-})] \quad (7)$$

$$\times [n_k^{j,+}(1-n_k^{j,+}) - n_k^{j,-}(1-n_k^{j,-})] \quad (8)$$

Here, $n_p^{i,\pm} = [\exp\{(E_p^i \mp \mu_i)/T\} + 1]^{-1}$ is the Fermi-Dirac distribution for flavor i with chemical potential μ_i and momentum mode p and m_i are the constituent quark masses, with $m_u = m_d = 340$ MeV or $m_s = 500$ MeV. The correlation function factorizes and can be written as:

$$\langle\Delta N^i\Delta N^j\rangle = \frac{G^2}{m_\sigma^2 T} \int_p F_p^i \int_p F_p^j \quad (9)$$

where we have defined:

$$F_p^i = \frac{2m_i}{E_p^i} [n_p^{i,+}(1-n_p^{i,+}) - n_p^{i,-}(1-n_p^{i,-})] \quad (10)$$

Here, we consider isospin symmetric case, $\mu_Q = 0$, which means $\mu_u = \mu_d = \mu_B/3$ and $\mu_s = \mu_B/3 - \mu_S$. Using chain rule to relate the correlation between fluctuations of quark flavors, u, d, s to fluctuations of conserved charges, B, Q, S , we obtain:

$$\chi_2^S = \int_p F_p^s \int_p F_p^s; \quad \chi_2^B = \frac{1}{9} (2 \int_p F_p^u + \int_p F_p^s)^2 \quad (11)$$

and if we consider $R(\mu_B, T) = \frac{\int_p F_p^u}{\int_p F_p^s}$, we obtain:

$$\chi_2^{S(crit)} = \frac{\chi_2^{B(crit)}}{\frac{4}{9}R(\mu_B, T)^2 + \frac{4}{9}R(\mu_B, T) + \frac{1}{9}} \quad (12)$$

We can estimate this ratio by considering values for $T_c, \mu_{B,c}$ consistent with current predictions for the critical point location, at $\mu_S = 0$ and $\mu_S = 0.25\mu_B$. For such predictions where $T = 100 - 120$ MeV and $\mu_B = 600 - 650$ MeV, we obtain $\chi_2^{S(crit)} \approx 0.3\chi_2^{B(crit)}$ in the $\mu_S = 0$ case, while in the strangeness neutral case, we get $\chi_2^{S(crit)} \approx 0.01\chi_2^{B(crit)}$. This means that in the latter case, the strangeness susceptibility is essentially insensitive to the possible presence of a critical point.

A natural question at this point is why proxies are needed rather than using the theoretically well-defined chiral susceptibility of the light quark flavors. The difficulty lies in the fact that the observables associated with light quarks have large finite volume effects as shown in Fig. 2. Consequently, determining the transition temperature and performing a reliable extrapolation to finite density would require larger lattice volumes. However, with larger volume, a remnant of the exponentially severe sign problem resurfaces in the Taylor based computation making the large chemical potential extrapolation prohibitively difficult. The problem can be understood as follows. Extrapolation to larger chemical potential requires higher order expansion coefficients. The terms making up the coefficient c_{2k} scale with volume as $\mathcal{O}(V^{k-1})$, whereas the c_{2k} itself remains finite in the thermodynamic limit ($V \rightarrow \infty$), being the expansion coefficient of an intensive quantity

like pressure. This implies large cancellations among the contributing terms and, consequently, a deteriorating signal-to-noise ratio of the coefficients with increasing volume and order. In contrast, the computation of the transition temperature based on strangeness susceptibility exhibits a much milder finite volume effect even if we reduce the simulation volume to $LT = 2$. This allows the use of smaller volumes with higher statistics, enabling the computation of higher-order Taylor coefficients and the extension of the analysis to larger values of μ_B/T .

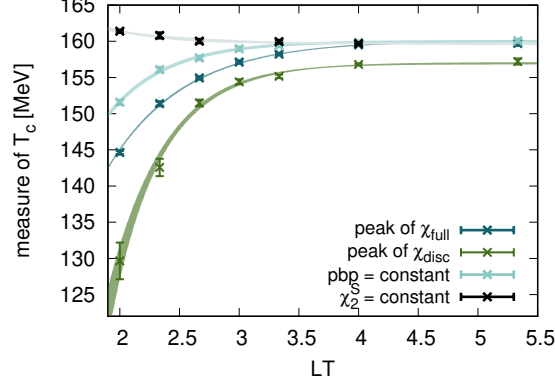


Figure 2: Different definitions and proxies for the QCD crossover temperature as functions of the lattice volume in temperature units (the aspect ratio) on $N_\tau = 12$ lattices. The measure of the transition temperature based on chiral observables have much larger finite volume effects than the definition based on strangeness fluctuations.

3. Simulation setup and Results

We use $N_f = 2 + 1$ flavors of rooted staggered fermions with 4 steps of HEX smearing [8] and the DBW2 action [9], at physical values of the quark masses. We employ two independent scale settings, one with the pion decay constant f_π and the other with a modified version of the Wilson-flow-based w_1 scale as introduced in [10], where this particular lattice action was already used. Both scale settings enter in the systematic analysis of our results. We use $16^3 \times 8$, $20^3 \times 10$ and $24^3 \times 12$ lattices to perform the continuum extrapolations of the transition line proxies up to $\mu_B = 400$ MeV. We have here the same statistics as in [10] on the $20^3 \times 10$ and $24^3 \times 12$, while on the $16^3 \times 8$ lattice, it is much larger. Additionally, we employ new simulation data set on a $24^3 \times 8$ lattice to gauge the finite volume effects (with 60000 – 70000 configurations per temperature). On the smaller lattices ($16^3 \times 8$ and $20^3 \times 10$), we use the reduced matrix formalism to calculate the fluctuations as was done in [10], whereas on the larger lattices we determine the μ_B -derivatives with stochastic sources [11].

In this study, we build a two-dimensional Taylor series expansion of the pressure in μ_B, μ_S as follows:

$$\frac{p(T, \mu_B, \mu_S)}{T^4} = \sum_{i,j=0}^{i+j=N} \frac{1}{i!j!} \chi_{ij}^{BS}(T) \mu_B^i \mu_S^j \quad (13)$$

where χ_{ij}^{BS} are the generalized baryon-strangeness susceptibilities. This allow us to write the strangeness number density and fluctuations at finite chemical potential as:

$$\chi_1^S(T, \mu_B, \mu_S) = \frac{\partial(p/T^4)}{\partial(\mu_S/T)} = \sum_{i=0, j=1}^{i+j=N} \frac{1}{i!(j-1)!} \chi_{ij}^{BS}(T) \mu_B^i \mu_S^{j-1} \quad (14)$$

$$\chi_2^S(T, \mu_B, \mu_S) = \frac{\partial^2(p/T^4)}{\partial(\mu_S/T)^2} = \sum_{i=0, j=2}^{i+j=N} \frac{1}{i!(j-2)!} \chi_{ij}^{BS}(T) \mu_B^i \mu_S^{j-2} \quad (15)$$

The order of the computation is set by the even integer, N where $N = 2$ corresponds to leading order (LO), $N = 4$ to next-to-leading order (NLO) and so on. We extrapolate the observables along the strangeness neutral line which is required to observe the collapse of the $\chi_{\bar{\psi}\psi, R}(\chi_2^S, \mu_B^I)$ curves in Fig. 1 and is also phenomenologically more relevant. For each (T, μ_B) pair, we search for $\mu_S = \mu_S^*$ that corresponds to the strangeness neutral case. In practice, we use Newton's method to iteratively solve for $\chi_1^S(\mu_S^*) = 0$ rather than Taylor expanding $\mu_S^*(\mu_B)$ itself. This approach achieves faster convergence in the orders of μ_B and yields both $\mu_S(T, \mu_B)$ and the susceptibility $\chi_2^S(T, \mu_B)$ simultaneously. We then construct the contours of $\chi_2^S = C$, where the constant $C \equiv \chi_2^S(T_0, \mu_{B,0})$ is the value this quantity takes at some reference temperature and chemical potential. The same procedure is applied to get the contours of constant μ_S/μ_B . We now turn to various systematics of Taylor based extrapolations to real chemical potential.

In Fig. 3, we show the extrapolated contours of constant μ_S/μ_B (left) and χ_2^S (right) starting from three reference temperatures from our $16^3 \times 8$ lattice. The contours span orders from NLO to N⁴LO in the Taylor expansion showing very good convergence. The effects beyond N²LO are visible only above $\mu_B \approx 450$ MeV, and a discrepancy between N³LO and N⁴LO appears, if at all, above $\mu_B \approx 500$ MeV. To sum up, we observe that up to $\mu_B \approx 400$ MeV, N²LO ($O(\mu_B^6)$) is consistent with higher orders for both contours.

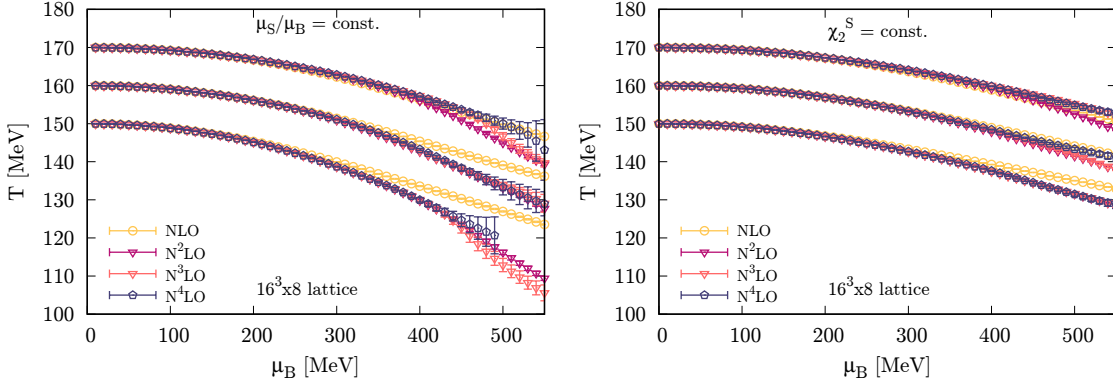


Figure 3: Contours of constant μ_S/μ_B (left) and χ_2^S (right) at different orders of the baryochemical potential in the Taylor expansion on the $16^3 \times 8$ lattice.

Since we are interested in the QCD transition proxies, we anchor the contours at the crossover temperature $T_c = 158$ MeV obtained at $\mu_B = 0$ in the continuum limit [3].

To assess the size of finite volume effects, we did the same analysis at N²LO order on the $24^3 \times 8$ lattice. In Fig. 4, the left plot shows resulting contours for the two volumes, $LT = 2$ and $LT = 3$ which suggests that finite volume effects are indeed small for the range covered using the

present statistics on the $24^3 \times 8$ lattice. Cut-off effects are probed by repeating the analysis at N²LO order for volume $LT = 2$ across $N_\tau = 8, 10, 12$ as shown in the right panel of Fig. 4.

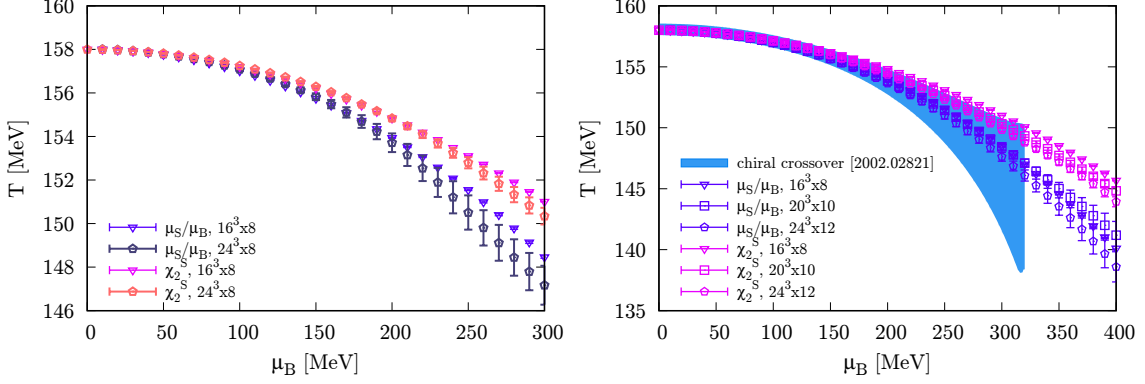


Figure 4: Left: Contours of constant μ_S/μ_B and χ_2^S at NNLO for $LT = 2, 3$. Right: Contours of constant μ_S/μ_B and χ_2^S at NNLO for $N_\tau = 8, 10, 12$ with $LT = 2$ compared with the chiral crossover results.

We observe that the two proxies differ slightly towards larger chemical potential although both are in agreement with the current continuum extrapolated result for the QCD crossover [3] with their spread smaller than the error on such result. The constant χ_2^S contours exhibit a systematic ordering with respect to N_τ which suggests a cutoff dependence. In contrast, for the constant μ_S/μ_B contours, no such ordering is observed for different N_τ and they are consistent with each other within the error indicating a very weak cutoff effect.

Finally, we perform the continuum extrapolation of the N²LO Taylor expansion results up to $\mu_B = 400$ MeV. In Fig. 5 we show this for the strangeness susceptibility (left) and μ_S/μ_B (right). We first observe, as noticed earlier, that cut-off effects are smaller for the latter, for which the results are almost N_τ -independent. In both panels, the two sets of points and fit bands indicate the results obtained with the two scale settings we employ. We consider the difference between the two scale settings as a source of systematic errors, and combine the two results in the following.

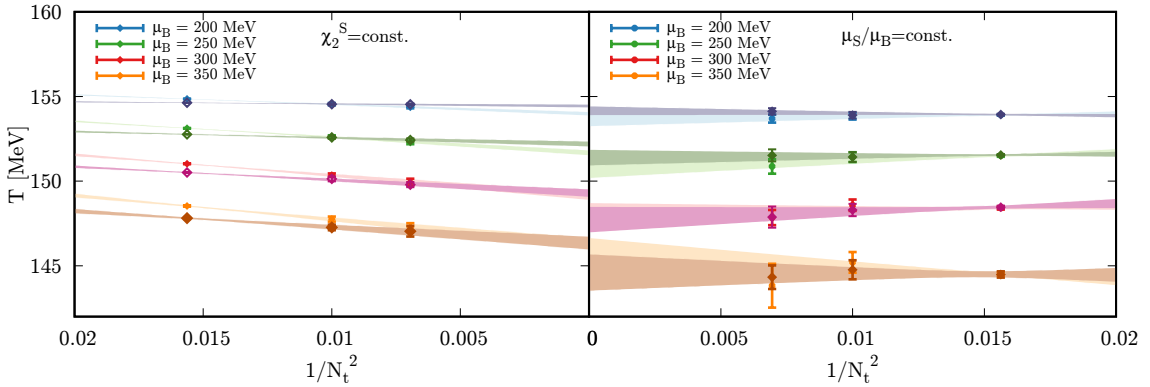


Figure 5: The continuum limit of the contours of constant χ_2^S and μ_S/μ_B for different values of the baryochemical potential. Here, lighter and darker colors correspond to the two scale settings employed in the analysis, namely, the f_π scale and the w_1 scale respectively.

4. Summary and Discussion

In this work we have shown how observables related to strangeness fluctuations can serve as proxies for the QCD transition and shed light on the phase structure of QCD at finite baryon chemical potential. Along the strangeness neutral line, the remarkable collapse of chiral susceptibility when plotted against χ_2^S and μ_S/μ_B as the μ_B^I is varied enables us to characterize the crossover with $\chi_2^S \approx 0.3$ and $\mu_S/\mu_B \approx 0.25$. We argued that the strangeness neutral condition suppresses the coupling of these proxies to the critical fluctuations in the vicinity of a critical point. We also observed that the finite volume corrections are under control even for $LT = 2$. We extrapolated the proxies to finite density using a two-dimensional Taylor series in (μ_B, μ_S) , and demonstrated convergence of the series at N²LO ($\mathcal{O}(\mu_B^6)$) up to $\mu_B \approx 400$ MeV. Finally, we continuum extrapolated these proxies as shown in the left panel of Fig. 6, being in perfect agreement with the chiral crossover line reported in [3]. The tension between the two proxies in the continuum is quite mild. In fact, the results coming from the two proxies can be taken together as the prediction for the crossover line interpreting their spread as the additional source of systematic error. Even then, the uncertainty is much smaller than what is known today as the chiral crossover line [3]. Additionally, we show the corresponding contours obtained from the Hadron Resonance Gas (HRG) model (using PDG16+ resonances), which agree strikingly well with our continuum extrapolations.

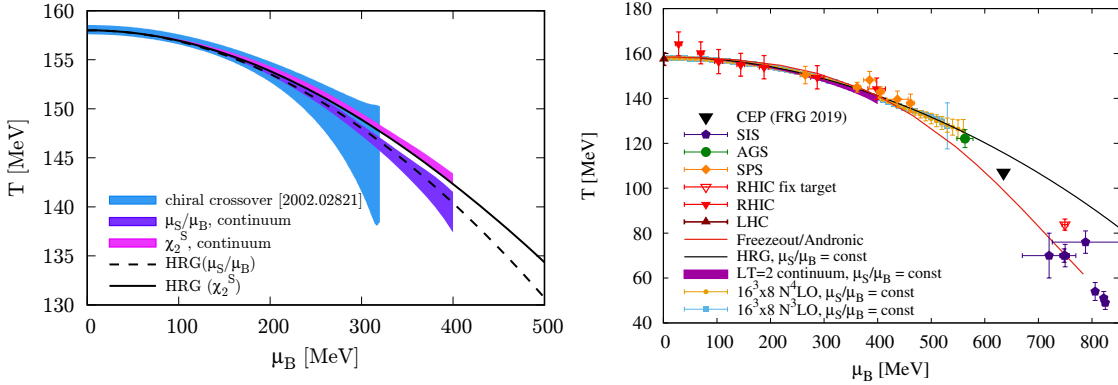


Figure 6: Left: Contours of constant μ_S/μ_B or χ_2^S from a N²LO Taylor expansion (constant values taken at $T_0 = 158$ MeV), extrapolated to the continuum, compared to the chiral crossover and to the HRG results. Right: Contours of constant μ_S/μ_B extended upto $\mu_B \approx 550$ MeV on $16^3 \times 8$ lattice.

The analysis of cut-off effects (Fig. 4 (right)) indicated that for μ_S/μ_B contours, our coarsest lattice, $16^3 \times 8$ is already close to the continuum limit. We thus extended the μ_S/μ_B contours for this lattice to N⁴LO i.e. including up to 10th order fluctuations to stretch the transition line beyond $\mu_B \approx 500$ MeV as shown in the right panel of Fig. 6. We also include the freeze-out data from various publications [12–16] along with their parametrization by [17] and a critical end point estimate from functional renormalization methods [18]. We stress that we have not demonstrated the validity of our proxies for the entire μ_B range. However, if we assume that they work, and that finite volume and discretization effects on $16^3 \times 8$ lattice data are under control, we may be guided by the HRG prediction and predict that the two curves start deviating between 400 and 500 MeV.

Acknowledgments

S.B and P.P. thank Jan M. Pawłowski and M. Stephanov for fruitful discussions. This work is supported by the MKW NRW under the funding code NW21-024-A. Z. Fodor acknowledges funding from the DOE under the contract number DE-SC0025025. This work was also supported by the Hungarian National Research, Development and Innovation Office, NKFIH Grant No. KKP126769. This work was also supported by the NKFIH excellence grant TKP2021_NKTA_64. This work is also supported by the Hungarian National Research, Development and Innovation Office under Project No. FK 147164. The authors gratefully acknowledge the Gauss Centre for Supercomputing e.V. (www.gauss-centre.eu) for funding this project by providing computing time on the GCS Supercomputer Juwels-Booster at Juelich Supercomputer Centre. We acknowledge the EuroHPC Joint Undertaking for awarding this project access to the EuroHPC supercomputer LUMI, hosted by CSC (Finland) and the LUMI consortium through a EuroHPC Extreme Access call. An award of computer time was provided by the INCITE program. This research used resources of the Argonne Leadership Computing Facility, which is a DOE Office of Science User Facility supported under Contract DE-AC02-06CH11357.

References

- [1] Y. Aoki, G. Endrodi, Z. Fodor, S. Katz and K. Szabo, *The Order of the quantum chromodynamics transition predicted by the standard model of particle physics*, *Nature* **443** (2006) 675 [[hep-lat/0611014](#)].
- [2] A. Bazavov et al., *Chiral crossover in QCD at zero and non-zero chemical potentials*, *Physics Letters B* **795** (2019) 15 [[1812.08235](#)].
- [3] S. Borsanyi, Z. Fodor, J.N. Guenther, R. Kara, S.D. Katz, P. Parotto et al., *The QCD crossover at finite chemical potential from lattice simulations*, *Phys. Rev. Lett.* **125** (2020) 052001 [[2002.02821](#)].
- [4] F. Gao and J.M. Pawłowski, *Chiral phase structure and critical end point in QCD*, *Phys. Lett. B* **820** (2021) 136584 [[2010.13705](#)].
- [5] P. Kovács, Z. Szép and G. Wolf, *Existence of the critical endpoint in the vector meson extended linear sigma model*, *Phys. Rev. D* **93** (2016) 114014 [[1601.05291](#)].
- [6] M.A. Stephanov, K. Rajagopal and E.V. Shuryak, *Event-by-event fluctuations in heavy ion collisions and the QCD critical point*, *Phys.Rev.* **D60** (1999) 114028 [[hep-ph/9903292](#)].
- [7] S. Borsányi, Z. Fodor, J.N. Guenther, P. Kumar, P. Parotto, A. Pásztor et al., *Finite density QCD phase structure from strangeness fluctuations*, [2510.26455](#).
- [8] S. Capitani, S. Durr and C. Hoelbling, *Rationale for UV-filtered clover fermions*, *JHEP* **11** (2006) 028 [[hep-lat/0607006](#)].
- [9] QCD-TARO collaboration, *Renormalization group flow of SU(3) gauge theory*, [hep-lat/9806008](#).

- [10] S. Borsanyi, Z. Fodor, J.N. Guenther, S.D. Katz, P. Parotto, A. Pasztor et al., *Continuum-extrapolated high-order baryon fluctuations*, *Phys. Rev. D* **110** (2024) L011501 [2312.07528].
- [11] C. Allton, S. Ejiri, S. Hands, O. Kaczmarek, F. Karsch et al., *The QCD thermal phase transition in the presence of a small chemical potential*, *Phys.Rev.* **D66** (2002) 074507 [hep-lat/0204010].
- [12] V. Vovchenko, V.V. Begun and M.I. Gorenstein, *Hadron multiplicities and chemical freeze-out conditions in proton-proton and nucleus-nucleus collisions*, *Phys. Rev.* **C93** (2016) 064906 [1512.08025].
- [13] F. Becattini, J. Steinheimer, R. Stock and M. Bleicher, *Hadronization conditions in relativistic nuclear collisions and the QCD pseudo-critical line*, *Phys. Lett. B* **764** (2017) 241 [1605.09694].
- [14] STAR collaboration, *Bulk Properties of the Medium Produced in Relativistic Heavy-Ion Collisions from the Beam Energy Scan Program*, *Phys. Rev. C* **96** (2017) 044904 [1701.07065].
- [15] V. Vovchenko, M.I. Gorenstein and H. Stoecker, *Finite resonance widths influence the thermal-model description of hadron yields*, *Phys. Rev. C* **98** (2018) 034906 [1807.02079].
- [16] A. Lysenko, M.I. Gorenstein, R. Poberezhniuk and V. Vovchenko, *Chemical freeze-out curve in heavy-ion collisions and the QCD critical point*, 2408.06473.
- [17] A. Andronic, P. Braun-Munzinger, K. Redlich and J. Stachel, *Decoding the phase structure of QCD via particle production at high energy*, *Nature* **561** (2018) 321 [1710.09425].
- [18] W.-j. Fu, J.M. Pawłowski and F. Rennecke, *QCD phase structure at finite temperature and density*, *Phys. Rev. D* **101** (2020) 054032 [1909.02991].